HHS Public Access

Author manuscript

J Biophotonics. Author manuscript; available in PMC 2019 November 01.

Published in final edited form as:

J Biophotonics. 2018 November ; 11(11): e201800053. doi:10.1002/jbio.201800053.

Measurement of Flow-Mediated Dilation of Mouse Femoral Artery *in vivo* by Optical Coherence Tomography

Weiye Song[1,‡], **Libo Zhou**[2,3,‡], **Kevin Liu Kot**[2], **Huijie Fan**[2], **Jingyan Han**[2,*], and **Ji Yi**[1,*]

[1]Department of Medicine, Boston Universty School of Medicine, Boston, MA, 02118, USA

[2]Vascular Biology Section, Evans Department of Medicine, Whitaker Cardiovascular Institute, Boston University School of Medicine, Boston, MA, 02118, USA

[3]State Key Laboratory on Integrated Optoelectronics, College of Electronic Science and Engineering, Jilin University, Changchun, Jilin, 130012, China

Abstract

Flow-mediated vasodilation (FMD) is used for assessment of vascular endothelial function in humans as a predictor of cardiovascular events. It has been challenging to carry it on preclinical murine models due to the diminutive size of the femoral artery. Here, we present a new approach to accurately measure the blood velocity and femoral artery diameters of mice by acquiring Doppler optical coherence tomography (DOCT) and optical coherence tomography angiography (OCTA) continuously within one single experimental scanning protocol. Using the high precision three-dimensional imaging and new velocity algorithm, the measurement precision of diameter, blood flow, velocity, and wall shear stress are improved to 0.91%, 11.0%, 10.7%, and 14.0%, respectively. FMD of healthy mouse femoral artery measured by this method was 11.96 ± 0.98%, which was blunted to 5.69±0.4% by intravenous administration of eNOS inhibitor (L-NAME), in agreement with that reported in the literature.

Graphical Abstract

Noninvasive estimation of flow-mediated dilation (FMD) in living mice is challenging mainly due to the diminutive size of mouse femoral artery since FMD was established in 1992. Here, we develop a new OCT-base image platform to measure FMD, wall shear stress, velocity, and blood flow in living mice by combining OCTA and Doppler OCT in one scanning protocol. OCT is thus a powerful technique to the assessment of mouse vascular function.

*Correspondence: jingyanh@bu.edu (J.H.), jiyi@bu.edu (J.Y.).

‡These authors contribute equally to this study.

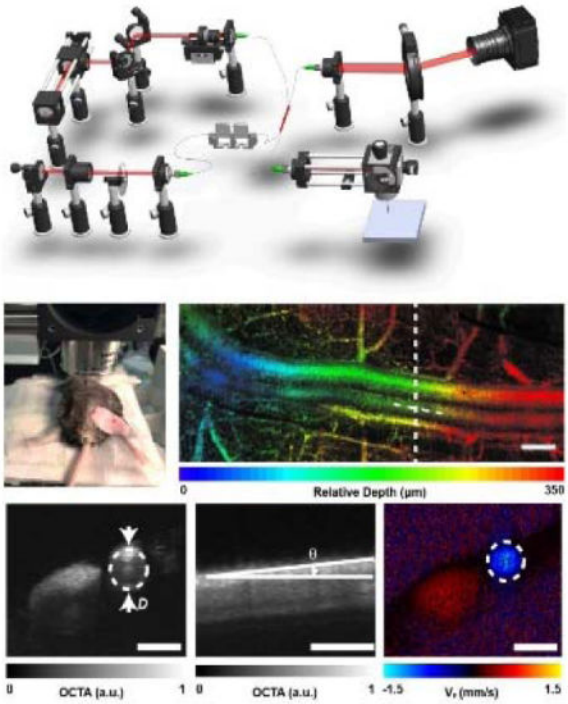

Keywords

optical coherence tomography; mouse femoral artery; flow-mediated dilation; arterial wall shear stress

Introduction

The endothelium, a single layer of cells lining the interior surface of the entire cardiovascular system, is by area alone, the largest organ that is indispensable for the maintenance of vascular homeostasis[1]. In response to shear stress imposed by blood flow, hormones, or neurotransmitters, healthy endothelial cells promote vascular function by production of vasoactive factors such as nitric oxide (NO) that maintain normal vascular tone and limit thrombosis and inflammation[2]. In contrast, the dysfunctioned endothelium under pathological conditions such as hypertension, obesity, and diabetes, initiate the development of atherosclerosis and thrombosis that are the primary pathological causes of the cardiovascular disease (CVD)[3]. Therefore, the vascular endothelial function is viewed as a barometer of vascular health estimating cardiovascular risk[4].

Given the utmost importance of endothelial function in the onset and progression of CVD, measurement of the endothelial function becomes a viable approach to estimate the patient's risk of the development of cardiovascular events. The measurement of flow-mediated dilation (FMD) has become the most widely used non-invasive method in clinic to gauge potential endothelial dysfunction since it was established in 1992[5]. In this FMD test on humans, ultrasound imaging is used to assess the vessel diameter and the blood flow before and after an increase in vessel wall shear stress (WSS) induced by reactive hyperemia, and

FMD is estimated with the percentage increase in vessel diameter from baseline. Over the past two decades, numerous clinical studies have shown that brachial artery FMD is positively correlated with vascular endothelial function and thus becomes a gold standard for assessment of arterial vascular function in clinical research[4]. However, noninvasive estimation of FMD in living mice, a highly desired experimental tool for studying vascular endothelial biology, is challenging mainly due to the diminutive size of mouse femoral artery. Recently, an elegant study of Schuler D. et al. characterized the physiology of FMD of mouse femoral artery that is measured by a method analogous to clinical FMD test with a high-frequent ultrasound imaging platform. The resultant FMD represents the local levels of active endothelial nitric oxide synthase (eNOS) and NO released from endothelial cells responding to shear stress and thus correlate with vascular endothelial function[6]. However, this method is technically demanding, as ultrasound imaging requires the transducer to be in acoustic contact with hindlimb without compressing vessels. The resolution and imaging speed of ultrasound limits the accurate estimation of dynamic changes of vessel diameters and blood flow. In addition, imaging a single cross section over a 3D femoral artery would introduce skew artifacts when the imaging plane does not precisely align with the center line of the vessel. This artifact will be especially challenging to overcome when acquiring dozens of images of mice femoral artery for several minutes *in vivo*. Therefore, these limitations of ultrasound stimulate the research seeking high resolution, high speed, three-dimensional imaging technique, as it can reduce the skew artifacts by recording the whole 3D blood vessel geometry and effectively reduce the operation difficulty and improve the measurement accuracy.

As an optical analog to ultrasound imaging with higher resolution, optical coherence tomography (OCT) is a non-contact optical imaging modality that provides three-dimensional imaging with micron-level resolution and millimeter level penetration[7]. OCT can utilize the Doppler effect to quantify blood flow velocity[8, 9]. The emerging OCT angiography (OCTA) provides high contrast and high sensitivity imaging of vasculature[10–12]. As a result, OCT is ideally suited for accurately estimating FMD in living mice. Here, we developed a new scanning protocol combining OCTA and Doppler OCT that continuously measures femoral artery vessel diameter, blood flow velocity, and wall shear stress every 10 seconds. Femoral artery shear stress is calculated using the velocity gradient along the radius of the vessel without the need for correction of phase wrapping occurred in Doppler OCT. In the test of FMD in mouse hindlimb, the vessel diameter, flow velocity, and wall shear stress of femoral artery are measured in real-time throughout the whole protocol. The FMD in healthy mice estimated with this new method is comparable to the result obtained using high-frequency ultrasound-based approach[6], and is significantly blunted by intravenous administration of eNOS inhibitor (L-NAME). These results together demonstrate that this OCT-based *in vivo* vascular imaging system is a new research tool for non-invasive, longitudinal, and precise assessment of vascular endothelial function in mice.

1. Materials and Methods

1.1. System setup

As shown in the schematic diagram of the OCT system (Figure 1a), a super-continuum laser (SuperK EXTREME, NKT Photonics) was used to generate a broadband laser output. The NIR portion (785–885 nm) was selected by two edge filters. The light was coupled into a 50/50 optical fiber coupler (FC), which distributed 50% of the incoming energy to the sample arm and the remaining energy to the reference arm. The light beam was collimated by an f=10 mm lens in the sample arm. Two galvanometer scanning mirrors (GVS102, Thorlabs) were used to steer the laser. An objective lens (LSM03, Thorlabs) was used to focus the laser. The reference beam was collimated and reflected by a mirror. A variable ND filter and several BK7 glass plates (DC) were installed in the reference arm to attenuate the light, and to compensate the dispersion in the sample arm, respectively. The returning light was sent to a customized spectrometer. A line scan camera (spL2048-140km, Basler) digitized the dispersed spectrum at a speed of 115 kHz, with 1024 pixel selected to output the spectrum, and the exposure time of the camera is 7 μs.

1.2. Image acquisition protocol

In order to simultaneously visualize the 3D structure of femoral artery and measure blood flow velocity during the FMD test, OCTA and Doppler OCT were combined within one single scanning protocol (Figure 1b). For OCTA, a sawtooth voltage with 80% duty cycle (Figure 1c) controlled the fast galvanometer. Four repeated B-scans were acquired at each location in the y-direction. Each B-scan contains 300 A-scans in the forward scanning direction. One OCTA volume contains 128 B-scans. For Doppler OCT, much denser sampling (3000 A-lines per B-scan in both forward and backward directions) was required to capture the phase shift between adjacent A-lines[9, 13]. The Doppler OCT collected 32 B-scans at the center location of the slow scanning direction. It took 1.7 s and 0.8 s to finish OCTA and Doppler OCT acquisition, respectively. After one sequence of the scan protocol, the data will be first saved to the computer RAM and then transformed to hard drive for further image reconstruction and analysis. The same acquisition protocol was then repeated every 10 s during the entire process of FMD. The incident power on the sample was ~2.5mW. The scanning range was 2×2 mm^2.

1.3. Animal Preparation

All procedures were approved by the Institutional Animal Care and Use Committee (IACUC) of Boston University Medical Center. We imaged the femoral artery of wild-type C57BL/6J mice (male at 8 weeks of age which were purchased from the Jackson Laboratory). Anesthetized mice introduced by intraperitoneal injection of Ketamine (80 mg/kg) and Xylazine (10 mg/kg) is placed on a heated examining plate to maintain the core body temperature at 37 ± 1°C during the whole procedure of FMD measurement. Epilated area of hindlimb is disinfected and a small incision (~1 mm) in the inner thigh is made to expose femoral artery, as shown in Figure 2a. To measure the FMD of the mouse in Figure 7, a vascular occluder (Fine Research Tools, #18080-03) is placed around the lower limb to induce occlusion of the femoral artery. Thirty minutes after the first FMD measurement, the same mouse was intravenously administrated with L-N^G-Nitroarginine methyl ester (L-

NAME, 8mg/kg of body weight) and underwent a second FMD test. Then the surgical adhesive will be applied to the small, non-tension bearing incisions and dissolve as the incision heals. Mice will be closely monitored post-operationally for evaluating incision healing and inflammation/infection. The inflamed areas will be treated with antibiotic ointments, and those intervention-resistant mice will be disqualified from experimental studies. The data presented in Figure 2 and Figures 4–6 were measured from different animals. For FMD measurements in Figure 7, the animal number was N=3, each producing control and L-NAME injection measurements.

1.4. Morphology measurements of mouse femoral artery by OCTA

The morphological metric of mouse femoral artery including vessel diameter and Doppler angle was measured from OCTA 3D dataset. Several preprocessing steps were first performed to generate OCT images, including normalizing the raw data by the light source spectrum, removing the DC spectral component, λ-k resampling, and digital dispersion compensation[13]. The morphological B-scan images were obtained by Fourier transform. After compensating the global axial phase shift, the subtractive difference was taken between adjacent complex B-scans, and the absolute values represented the angiographic signal[12, 14]. A three-dimensional median filter (3×3×3 pixels) was then applied to the OCTA dataset to improve the image quality. A representative depth-encoded OCTA image is shown in Figure 2b. The blood vessel diameter then can be manually measured by cross sectional OCTA image (Figure 2c). The measurement criterion is based on the best visual fit of the circle to the vessel lumen. The waisted double fan-shaped intensity pattern inside the artery is due to the orientation of the red blood cells toward laminar shear flow[15, 16]. A cardic cycle is easily recognizable from *en face* OCTA images as the systolic period will cause artefacts as vertical lines, as shown in Figure 4. The subsequent diastolic period generally has a better OCTA image quality, and the vessel diameter does not change significantly. Therefore, the measurement of diameter was taken from one single OCTA B-scan image during a diastolic period. We also measured the Doppler angle θ of the vessel geometrically for subsequent blood flow calculation by extracting the cross-sectional OCTA image along the centerline of the femoral artery as shown in Figure 2d.

1.5. Blood flow measurements by Doppler OCT

To measure the blood flow, the phase contrast $\Delta\phi$ between two adjacent A-lines was first used to extract Doppler projective blood velocity v_p, along the beam direction by [9, 17, 18],

$$v_p = \frac{f_{sample} \cdot \lambda_0 \cdot \Delta \varnothing}{4 \cdot \pi \cdot n}, \quad (1)$$

Where f_{sample} is the OCT A-line scanning frequency, which is 115 kHz in our system; λ_0 (nm) is the central wavelength of the OCT light source; n is the refraction index of the sample, assumed to be 1.38. The absolute blood velocity is then

$$v = \frac{v_p}{\sin\theta}, \quad (2)$$

where θ is the angle defined as in Figure 2d. The total blood flow F (μL/s) is equal to the product of the velocity and the vessel cross-sectional area

$$F = v \times \frac{\pi}{4} \cdot D^2, \quad (3)$$

Where D is the diameter of blood vessel. The velocity and flow measurements averaged thirty-two B-scans from the Doppler OCT acquisition, covering 0.8s for roughly 4 cardiac cycles.

1.6. Wall shear stress calculation

WSS was calculated by the following equation assuming a laminar flow in femoral artery[6]

$$\mathrm{WSS} = 8 \times \mu \times \mathrm{v_m/D}, \quad (4)$$

where v_m is mean velocity and blood viscosity (μ) was assumed to be constant at 0.035 dyne×sec/cm^2.

The above equation is only applicable when there is no phase wrapping. When there is significant phase wrapping and washout effect as a consequence of high blood flow rate in the femoral artery, we use the following formulations to calculate WSS and velocity instead. The parabolic velocity profile for the laminar flow is

$$\mathrm{v(r)} = \mathrm{v_{max}}\left[1 - \left(\frac{2\mathrm{r}}{\mathrm{D}}\right)^2\right], \quad (5)$$

where $\mathrm{v_{max}}$ is the maximum velocity in the center of the vessel, r is the radial distance from the vessel center, and D is the vessel diameter. We obtained $\mathrm{v_{max}}$ by fitting the velocity profile with the parabolic equation. The mean velocity is the integration of the velocity over the cross sectional area of the vessel Q, divided by the cross sectional area A,

$$v_m = Q/A = \int_0^{\frac{D}{2}} v(r) 2\pi r dr \Big/ \pi\left(\frac{D}{2}\right)^2. \quad (6)$$

After plugging Eq. (5) into Eq. (6), the mean velocity is equal to half of the maximum velocity, $v_m=v_{max}/2$. Then WSS was calculated by

$$\mathrm{WSS} = 4 \times \mu \times \frac{v_{max}}{D}. \quad (7)$$

When phase wrapping occurs, the fitting only applies to the rising segment of velocity profile without the need to un-wrap the phase.

2. Results

We first characterized the roll-off performance of our system. A silver mirror was placed in the sample arm and imaged over a range of depths. To mimic the signal level backscattered from tissue, an OD=2 neutral density filter was used to attenuate the light in the sample arm. Figure 3a shows the roll-off curves measured in our system. The sensitivity is estimated to be ~80 dB, taking into account the 40dB attenuation of the neutral density filter. The roll-off rate was about 6dB/mm. The axial resolution was measured to be ~7.5 μm from the first peak. The lateral resolution is measured to be ~8.2 μm by imaging the sharp edge of a razor blade.

We next characterized the accuracy of the flow velocity measurement. As the diameter of mouse femoral artery is around 250 μm, a transparent plastic tube with an inner diameter of 250 μm was used to simulate the blood vessel. A milk phantom diluted 1:1 by water was used to simulate the blood and pumped through the tube. A syringe pump was used to precisely control the flow speed. The tube was mounted on a stage to keep the Doppler angle consistent, and the Doppler angle was measured from the 3D OCT image of the tube to calculate the projective velocity. The scanning protocol was the same as described in the method section. The phase contrast was recorded at different velocities. Figure 3b shows an excellent correlation between the present and measured projective velocity with R^2=0.9994 by a linear regression. Thirty-two repeated measurements were taken at each speed and all the standard deviations of the measurements were within 0.06 mm/s.

After characterizing the system performance, the scanning protocol was tested on a health femoral artery without performing FMD. Figure 4a and 4b show two *en face* projections of OCTA collected 150 s apart. A translocation of the imaging region between two time points is apparent by the shift of the branching vessels, due to the slight movement. As shown in Figure 4b, when the same frame of B-scan in OCTA (white dash line) was used to calculate vessel diameter, the translocation would cause measurement error due to the intrinsic variation in the vessel diameter. Thanks to the 3D capability of OCTA, we took the vessel branching point (green dots) as the reference to reliably and accurately measure the vessel diameter at the identical location, avoiding the measurement error due to the translocation. The benefit of using the reference is more clearly shown in Figure 4c. When we analyzed 30 consecutive vessel diameter measurements every 10s from OCTA, without and with the branching vessel as the reference, the relative standard deviation (RSD) reduced from 4.0% to 0.7%. By using the 3D OCTA image, the vessel diameter can be accurately measured.

Next, we validated our measurements of blood flow and WSS. The phase shifts between the adjacent A-line OCT signal reflect the projective velocity, v_p (mm/s), along the beam axis. Therefore, phase wrapping appears when either the Doppler angle or the blood flow was large. Although the angle of mouse's femoral artery was adjusted prior to each measurement, phase wrapping was still often present during the whole measurement. Instead of correcting the phase wrapping, we used the velocity gradient with respect to the distance to the vessel central axis to calculate blood flow and WSS.

Figure 5a–d show an example of blood flow and WSS calculation without phase wrapping. The OCTA image provides the vessel diameter (Figure 5a). The Doppler OCT images in Figure 5b show the typical parabolic flow pattern. The depth profile of v_p is shown in Figure 5c by averaging the signal within the yellow dashed area. When we used the raising range of v_p to fit Eq. (5), the parabolic profile and the actual v_p had an excellent agreement. Then the blood flow could be calculated according to Eq. (2). To further validate our method, we compared our method with the conventional method of calculating blood flow, which takes the mean value of v_p within the vessel. Two methods match well with each other over ~4 pulsatile flow pattern due to cardiac cycle within 0.83s acquisition time, with averaged blood flow to be 0.245 and 0.239 mL/min, respectively. Figure 5e–h show the measurements on the same femoral artery 150s later, when the phase wrapping occurred (Figure 5f). The depth profile of v_p from the direct measurements is plotted in Figure 5g, as the black curve. When the rising segment of v_p was used to fit Eq. (5), the parabolic pattern is shown in red curve. We then further calculated the blood flow using our fitting method, giving an averaged blood flow as 0.231 mL/min, which is consistent with previous measurements in Figure 5d. In contrast, the conventional method without phase wrapping compensation would result in a significant underestimation. Based on the measurement of blood velocity, WSS could also be calculated by Eq. (4).

After verifying our method of measuring blood vessel diameter, blood flow, and WSS, we analyzed the variation of the four parameters over the consecutive 30 measurements (every 10 s for 5 mins in total) at three different locations (L_1, L_2 and L_3) from upper to lower stream along the same femoral artery. The RSDs were within 0.8%, 0.91% and 0.71% for vessel diameter at three locations, with L_1 and L_2 being the thickest and thinnest (Figure 6a). Since the measurements were taken from the same vessel, the flow were maintained independent of vessel diameter as in Figure 6b; and the RSDs were within 10.2%, 11.0%, and 4.7%, at three locations, respectively. The constant blood flow resulted in larger velocity at thinner vessel as shown in Figure 6c. The higher velocity and smaller vessel size also resulted in larger WSS as indicated in Figure 6d. The RSDs are 9.8%, 10.7%, and 4.9% for velocity; and 9.7%, 14.0%, and 5.1% for WSS at three locations respectively. The values of blood vessel diameter and blood flow velocity from our measurements are consistent with the previous reports[6, 19].

As FMD is almost entirely mediated by eNOS, the high precision and effectiveness of measuring FMD were demonstrated by the result that the FMD % value was markedly blunted after intravenous administration of L-NAME (a competitive NOS inhibitor). The femoral artery was first occluded for 3 minutes with an inflatable cuff on the lower leg, and the subsequent hemodynamic response was continuously measured every 10 seconds after

releasing the cuff. FMD% value was quantified as the percent change of the diameter after releasing the cuff as compared to pre-release values: FMD = [($D_{\text{after-release}} - D_{pre\text{-}release}$)/$D_{pre\text{-}release}$]×100%. As shown in Figure 7, 'B' represented the baseline data before the cuff releasing, and other data were acquired during a period of 5 minutes after deflation. We can see the blood flow immediately increased after releasing and gradually recovered to the baseline. The dilation of the vessel peaked around 140s and WSS generally followed the trend of blood flow. Our results show that the average FMD was 11.96±0.98%, which was robustly reduced to 5.69±0.4% by intravenous administration of L-NAME. Of note, the WSS, but not the flow velocity was significantly decreased by L-NAME treatment.

3. Discussion

FMD test has been established for over two decades as a reliable measurement of vascular endothelial function in humans and widely used in clinics assessing the risk for cardiovascular events[5, 20] However, until recently, Schuler D. et. al characterized the physiology of FMD of the femoral artery in living mice, the most useful and valid animal model for studying cardiovascular disease[6]. In a series of elegant studies, they provided definitive evidence that, analogous to FMD in humans, vasodilation occurs following ischemia-induced reactive hyperemia, which is primarily mediated by activation of eNOS and subsequent NO production, representing endothelial function. The measurement accuracy of the blood arterial diameter and shear rate is a key for FMD calculation. In the present study, OCT-based imaging technique with features of contact-free, label-free, and high resolution is employed to estimate FMD. The imaging protocol combines the OCTA and Doppler OCT to measure vessel diameter and blood flow. Although Doppler OCT can measure the diameter of the blood vessel, herein, angiography data was chosen to measure the diameter due to the following reasons. First, blood flow in the femoral artery is considered as laminar flow in which the layer in contact with a stationary surface has minimum velocity and increases towards the vessel center. Thus, the flow velocity at vessel wall is too low to get a reliable Doppler signal especially at the end of diastole[21]. In contrast, OCTA is much more sensitive to the slow blood flow and measures blood vessel more accurately. Second, the scanning density in OCTA is more sparse than Doppler OCT so that it can provide a 3D structure of femoral vessels in mouse hindlimb, which enables identifying the same location of the blood vessel during an FMD test. The limitation of OCTA is lack of absolute measurement of blood flow, which is complemented by the Doppler OCT measurement. In our current setup, a total scan time duration of 0.8s allows Doppler OCT imaging of the femoral artery over about 4 cardiac cycles. The averaged blood flow should avoid the pulsatile blood flow pattern.

To calculate blood flow velocity, we used a parabolic fitting to estimate the mean velocity and WSS instead of a conventional phase un-wrapping method. This is because the high flow speed in the femoral artery often caused several phase wrapping within a vessel and the un-wrapping method can become complicated. Therefore, after verifying that the parabolic fitting has a good precision as shown in Figure 5, we used it to calculate the blood velocity in this study.

As the wall shear stress exerted on endothelium is the primary stimulus for FMD response, it is imperative to accurately estimate the blood velocity and shear rate during FMD test, which is a significant challenge in mice due to the small size of hindlimb and femoral artery. In this context, OCT-based imaging system demonstrates a clear contact-free advantage over ultrasound technique. In ultrasound, it requires the optimal insonation angle and size of the sample volume by appropriately placing the probe to acoustically contact mouse femoral artery but not compress the vessels. In OCT, the direct contact is completed eliminated.

Normalizing FMD by the shear rate has been thought to eliminate the impact of heterogeneous reactive hyperemia across healthy young/old subjects and those with peripheral vascular diseases[22–25]. As the diameter and WSS of blood vessel can be measured in one scanning protocol by using OCT-based image platform, we can envision that using this method, the FMD in mice may be accurately estimated and well correlated with vascular endothelial function by, 1) obtaining the true peak diameter and expressing as an increase in vasodilation above baseline values, 2) normalizing FMD for shear rate area under the curve, which is necessary to alleviate the impact of alteration in reactive hyperemia particularly in mouse models of aging and peripheral artery diseases.

In the current study, to obtain the 3D structural and functional images with 1.3 μm resolution and 1mm depth penetration, a small (1mm) incision on hindlimb of mice was made to expose the femoral artery. Although its impact on FMD test is neglectable, for the further improvement, a 1300 nm system may be used to render a better penetration achieving a genuinely non-invasive vascular imaging system.

4. Conclusion

To the best of our knowledge, this study is for the first time to establish an OCT-based imaging system combining OCT angiography and Doppler components for accurate assessment of FMD of mouse femoral artery, a reliable, *in vivo* measurement of vascular endothelial function. The current OCT system enables three-dimensional imaging of anatomy with micron-level resolution. We developed a scanning protocol allowing to acquire the 3D structure of femoral artery, blood flow velocity, and WSS every 10 seconds continuously within one single volumetric scan. The high precision in measurement of vessel diameter and WSS can render accurate estimation of FMD and associated endothelial function that is evidenced by the fact of FMD inhibition by eNOS inhibitor.

Acknowledgments

This study is supported by Evans medical foundation (to J. Y.), BU CTSI KL2TR001411 (to J. Y.), American Heart Association 14SDG20140036 (to J. H.), and NIH R56HL130194 (to J.H.)

References

1. Galley HF, Webster NR. Brit J Anaesth. 2004; 93:105–113. [PubMed: 15121728]
2. Khazaei M, Moien-Afshari F, Laher I. Pathophysiology. 2008; 15:49–67. [PubMed: 18434105]
3. Davignon J, Ganz P. Circulation. 2004; 109:27–32.
4. Vita JA, Keaney JF. Circulation. 2002; 106:640–642. [PubMed: 12163419]

5. Celermajer DS, Sorensen KE, Gooch VM, Spiegelhalter DJ, Miller OI, Sullivan ID, Lloyd JK, Deanfield JE. Lancet. 1992; 340:1111–1115. [PubMed: 1359209]
6. Schuler D, Sansone R, Freudenberger T, Rodriguez-Mateos A, Weber G, Momma TY, Goy C, Altschmied J, Haendeler J, Fischer JW, Kelm M, Heiss C. Arterioscl Throm Vas. 2014; 34:2651–U2176.
7. Huang D, Swanson E, Lin C, Schuman J, Stinson W, Chang W, Hee M, Flotte T, Gregory K, Puliafito C, et al. Science. 1991; 254:1178–1181. [PubMed: 1957169]
8. Izatt JA, Kulkarni MD, Yazdanfar S, Barton JK, Welch AJ. Opt Lett. 1997; 22:1439–1441. [PubMed: 18188263]
9. Zhao Y, Chen Z, Saxer C, Xiang S, de Boer JF, Nelson JS. Opt Lett. 2000; 25:114–116. [PubMed: 18059800]
10. Wang RK, Jacques SL, Ma Z, Hurst S, Hanson SR, Gruber A. Opt Express. 2007; 15:4083–4097. [PubMed: 19532651]
11. Chen CL, Wang RK. Biomed Opt Express. 2017; 8:1056–1082. [PubMed: 28271003]
12. Yi J, Chen S, Backman V, Zhang HF. Biomed Opt Express. 2014; 5:3603–3612. [PubMed: 25360376]
13. Wojtkowski M, Srinivasan VJ, Ko TH, Fujimoto JG, Kowalczyk A, Duker JS. Opt Express. 2004; 12:2404–2422. [PubMed: 19475077]
14. Chen S, Yi J, Zhang HF. Biomed Opt Express. 2015; 6:2840–2853. [PubMed: 26309748]
15. Cimalla P, Walther J, Mittasch M, Koch E. J Biomed Opt. 2011; 16
16. Bernucci MT, Merkle CW, Srinivasan VJ. Biomed Opt Express. 2018; 9:1020–1040. [PubMed: 29541501]
17. Wang YM, Bower BA, Izatt JA, Tan O, Huang D. J Biomed Opt. 2007; 12
18. Leitgeb RA, Schmetterer L, Drexler W, Fercher AF, Zawadzki RJ, Bajraszewski T. Opt Express. 2003; 11:3116–3121. [PubMed: 19471434]
19. Hong GS, Lee JC, Robinson JT, Raaz U, Xie LM, Huang NF, Cooke JP, Dai HJ. Nat Med. 2012; 18:1841–1846. [PubMed: 23160236]
20. Corretti MC, Anderson TJ, Benjamin EJ, Celermajer D, Charbonneau F, Creager MA, Deanfield J, Drexler H, Gerhard-Herman M, Herrington D, Vallance P, Vita J, Vogel R. J Am Coll Cardiol. 2002; 39:257–265. [PubMed: 11788217]
21. Cimalla P, Walther J, Mittasch M, Koch E. J Biomed Opt. 2011; 16
22. Huang AL, Silver AE, Shvenke E, Schopfer DW, Jahangir E, Titas MA, Shpilman A, Menzoian JO, Watkins MT, Raffetto JD, Gibbons G, Woodson J, Shaw PM, Dhadly M, Eberhardt RT, Keaney JF, Gokce N, Vita JA. Arterioscl Throm Vas. 2007; 27:2113–2119.
23. Wray DW, Uberoi A, Lawrenson L, Richardson RS. Am J Physiol-Heart C. 2006; 290:H1271–H1277.
24. Pyke KE, Tschakovsky ME. J Appl Physiol. 2007; 102:1510–1519. [PubMed: 17170205]
25. Padilla J, Johnson BD, Newcomer SC, Wilhite DP, Mickleborough TD, Fly AD, Mather KJ, Wallace JP. Cardiovasc Ultrasound. 2008; 6

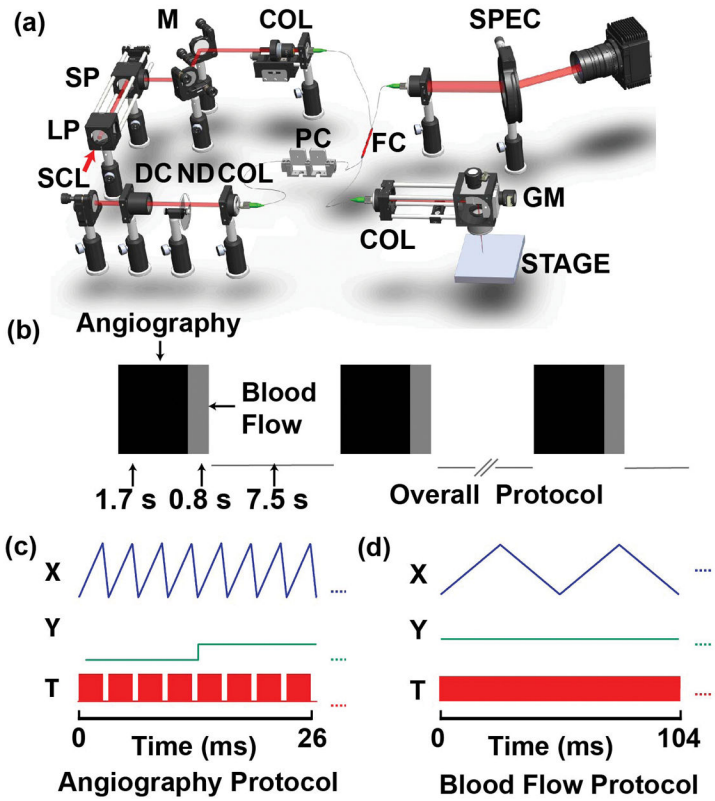

Figure 1.

The schematic and the scanning protocol of the OCT system. (a) The OCT system. SCL: super-continuum laser. LP: long pass dichroic mirror. SP: short pass dichroic mirror. M: a mirror. COL: collimator. FC: fiber coupler. PC: polarization controller. DC: dispersion control glass. ND: Neutral Density. GM: galvanometer mirror. (b) The OCT scanning protocol. (c)–(d) Triggering signals for acquiring angiography and flow data, respectively. The X and Y waveforms are the signals for triggering two galvanometer mirrors, respectively. The T waveforms are the signals for triggering the spectrometer. In (c), each red block contains 300 triggers within one OCT B-scan. In (d), there are 3000×4 triggers in the red block, with each B-scan composed of 3000 A-lines.

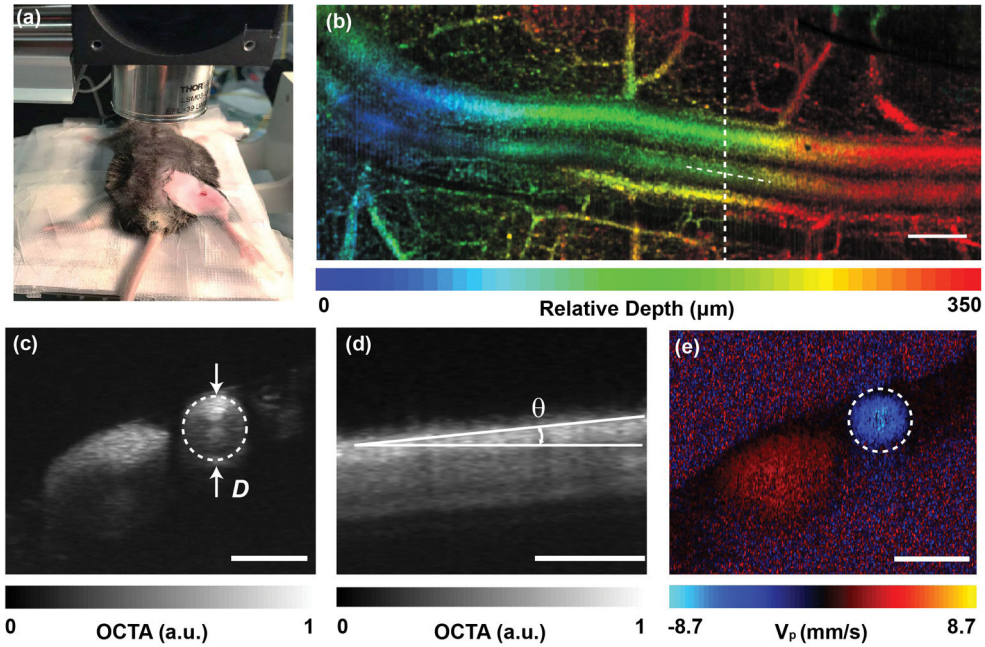

Figure 2.

The *in vivo* imaging of a mouse femoral artery. (a) The photograph is showing the location of the incision over the femoral artery. (b) *In vivo* depth-encoded *en face* view of OCTA from a mouse femoral artery. The image is stitched by three volumetric data sets. (c) The diameter of the blood vessel. (d) The Doppler angle of the blood vessel, measured from the cross-sectional OCTA image along the blood vessel centerline depicted in (b). (e) The Doppler phase-contrast image is showing the projective blood flow velocity along the beam axis. Panel (c) and (e) are roughly at the same B-scan location. Bar =300 μm.

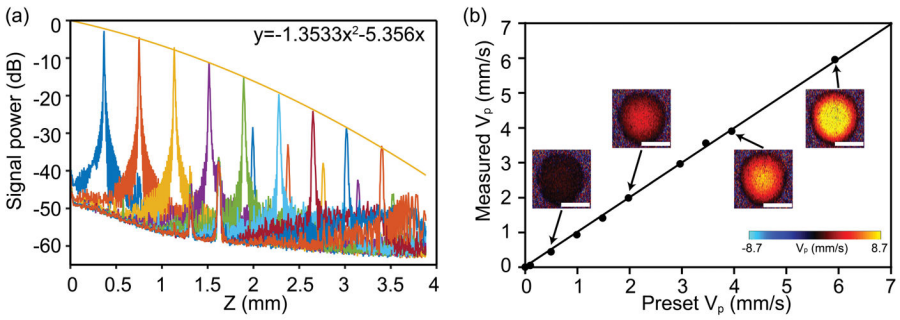

Figure 3.

System characterization. (a) The roll-off performance of our system. A second-order polynomial fitting was provided. The roll-off rate is about 6 dB/mm. The secondary peak is an artefact due to the specular reflection from the mirror in the sample arm. (b) The projective flow velocity v_p calibration by a blood flow phantom composed of 1:1 diluted milk pumped through a capillary tube. The flow velocity was precisely controlled by a syringe pump. The examples of the DOCT B-scan images of capillary tube was shown at various speeds. The averaged phase contrast within the tube was used to calculate v_p. Bar =150 μm.

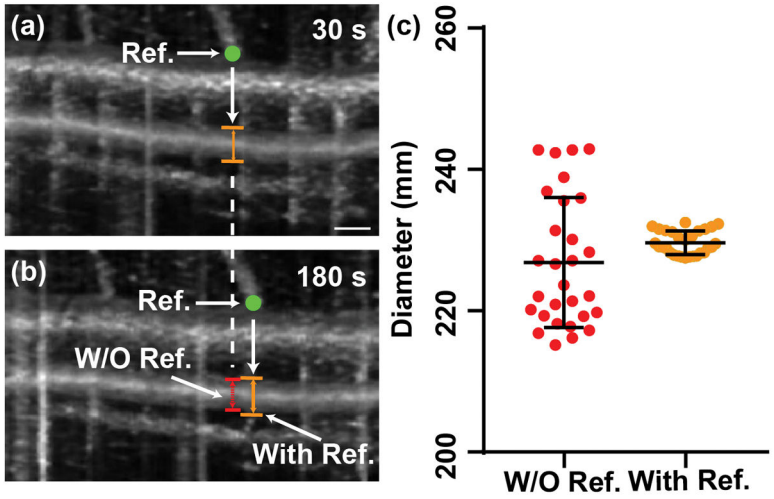

Figure 4.

(a–b) Two *en face* projections of OCTA over the same femoral artery that was acquired 150 s apart. The location of a branching vessel was chosen to be the reference point (the green point) and to offset the slight displacement. The vessel diameter was measured underneath the reference point, as we called OCTA measurement with reference. In panel (b), the red line is the same B-scan location in the OCTA image without reference. The vertical lines in panel (a) and (b) were caused by the cardiac cycles. Bar = 0.2 mm. (c) The measurements of blood vessel diameter from 30 consecutive volumetric scans of the same femoral artery over 5 minutes, with and without reference, respectively. Error bars are standard deviation.

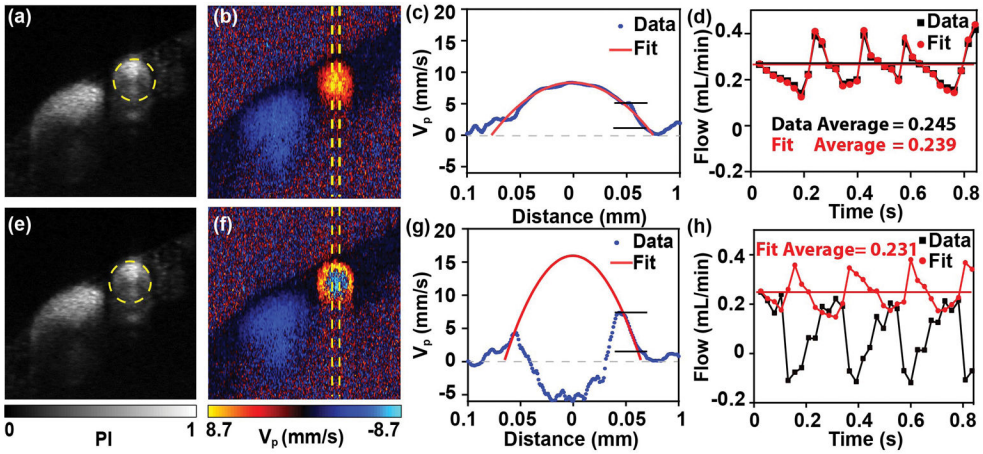

Figure 5.

(a, e) The cross-sectional OCTA images of the femoral artery without and with phase wrapping. (b, f) The corresponding Doppler phase contrast images of the femoral artery without and with phase wrapping. (c, g) The projective blood flow velocity as a function of the distance from the central axis of the blood vessel, without and with phase wrapping. The velocity was averaged within the central regions of the femoral artery labeled in (b). The blue line is the raw result and the red line is the fitting result fitted from the raw parts over the rising segment of the velocity under a laminar flow assumption. (d, h) The calculated blood flow rates indicating cardiac cycles, without and with phase wrapping. The black line was calculated from integrating the raw phase shift signals within the blood vessel, and the red line was calculated from the fitting result. The horizontal lines are the mean results.

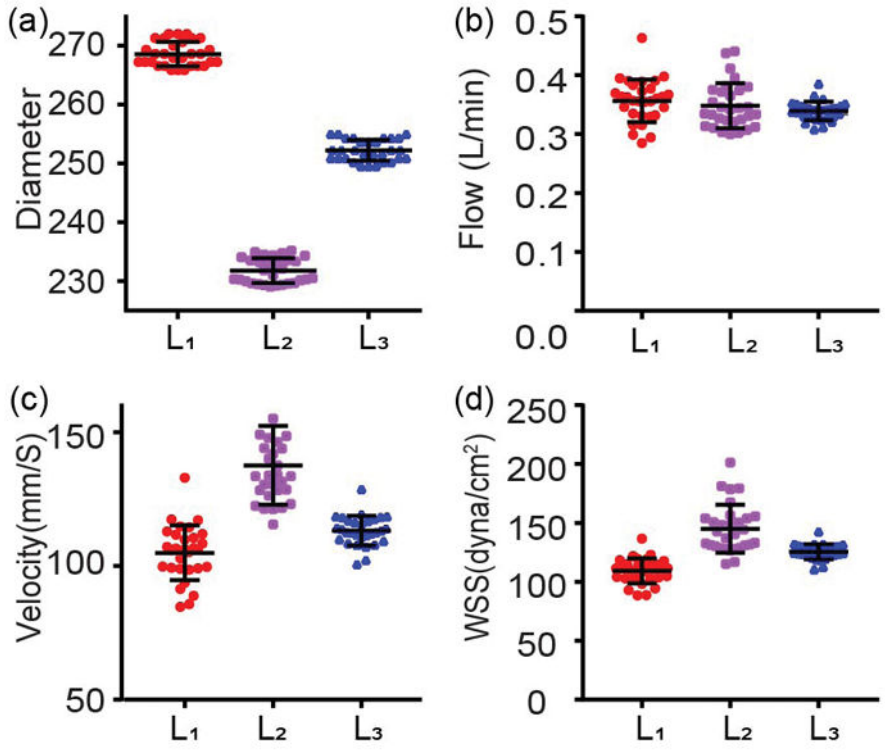

Figure 6.

The precision analysis of measurements of blood vessel diameter in (a), blood flow in (b), blood flow rates velocity in (c), and WSS in (d). The WSS was measured 30 times consecutively over 5 times. All the data was acquired from the same femoral artery *in vivo*. The interval of each acquisition is 10 s. L_1, L_2, L_3 in each figure indicate three different locations along the artery. Error bar = stander deviation.

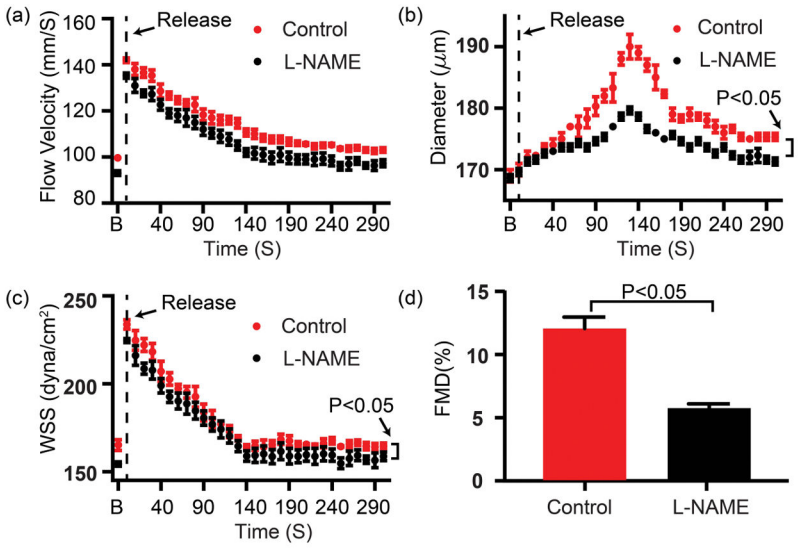

Figure 7.

In vivo measurement of (a) Flow velocity, (b) Diameter, (c) WSS, (d) FMD% of healthy C57BL6J mice undergoing FMD test described in the Methods without and with L-NAME intravenous administration. the horizontal axis is the time after releasing the cuff; the 'B' representative baseline data prior to occlusion. The black curve and the red curve represent the vessel responses before and after L-NAME intravenous adminstration. $p < 0.05$, n=3. Error bar = standard deviation.